Research Article | Vol. 26, No. 13 | 25 Jun 2018 | OPTICS EXPRESS 17254
Optics EXPRESS

Theoretical modeling and analysis on the absorption cross section of the two-photon excitation in Rb

HANGHANG YU,[1,2] FEI CHEN,[1,*] YANG HE,[1] SHAO ZHANG,[1,2] QI-KUN PAN,[1] DEYANG YU,[1] AND JIJIANG XIE[1]

[1]*State Key Laboratory of Laser Interaction with Matter, Innovation Laboratory of Electro-Optical Countermeasures Technology, Changchun Institute of Optics, Fine Mechanics and Physics, Chinese Academy of Sciences, 3888 Dongnanhu Road, Changchun Jilin 130033, China*
[2]*University of Chinese Academy of Sciences, Beijing 100049, China*
[*]*feichenny@126.com*

Abstract: The cross-section is crucial for quantitative characterization and analysis of the absorption process. A model on the absorption cross-section of the simultaneous two-photon excitation in Rb-vapor four-wave mixing process is established by using the coupled-wave equation. Taken into account of the hyperfine structures for ^{85}Rb and ^{87}Rb, the third-order susceptibility and hyperfine line strength are calculated respectively. Then, the influences of hyperfine transition on cross section are investigated and simulation results agree well with the experiment results. The calculated results suggest that high pumping power intensity is essential in Rb two-photon excitation, while narrow linewidth is the limiting factor of high absorption efficiency by comparing normalized absorption profile between pumping beam and two-photon excitation process. Additionally, two approaches to improving absorption efficiency, linewidth narrowness of the pumping beam and absorption linewidth broadening, are proposed.

OCIS codes: (140.1340) Atomic gas lasers; (140.3430) Laser theory; (190.4180) Multiphoton processes; (020.2930) Hyperfine structure.

References and links

1. B. H. Cumpston, S. P. Ananthavel, S. Barlow, D. L. Dyer, J. E. Ehrlich, L. L. Erskine, A. A. Heikal, S. M. Kuebler, I. Y. S. Lee, and D. Mccordmaughon, "Two-photon polymerization initiators for three-dimensional optical data storage and microfabrication," Nature **31**, 52 (1999).
2. W. R. Zipfel, R. M. Williams, and W. W. Webb, "Nonlinear magic: multiphoton microscopy in the biosciences," Nat. Biotechnol. **21**(11), 1369–1377 (2003).
3. W. K. Kaiser and C. G. B. Garrett, "2-Photon Excitation in Caf_2 - Eu^{2+}," Phys. Rev. Lett. **7**(6), 229–231 (1961).
4. M. Göppert-Mayer, "Über Elementarakte mit zwei Quantensprüngen," Ann. Phys.-Berlin **401**(3), 273–294 (1931).
5. G. Grynberg and B. Cagnac, "Doppler-free multiphotonic spectroscopy," Rep. Prog. Phys. **40**(7), 791–841 (1977).
6. M. Marinescu, V. Florescu, and A. Dalgarno, "Two-photon excitation of the 5 ^{2}D states of rubidium," Phys. Rev. A **49**(4), 2714–2718 (1994).
7. A. M. Akulshin, A. A. Orel, and R. J. Mclean, "Collimated blue light enhancement in velocity-selective pumped Rb vapour," J. Phys. At. Mol. Opt. Phys. **45**(1), 015401 (2012).
8. A. M. Akulshin, N. Rahaman, S. A. Suslov, and R. J. Mclean, "Amplified spontaneous emission at 5.23 um in two-photon excited Rb vapour," J. Opt. Soc. Am. B **34**(12), 2478 (2017).
9. M. P. Moreno, G. T. Nogueira, D. Felinto, and S. S. Vianna, "Two-photon transitions driven by a combination of diode and femtosecond lasers," Opt. Lett. **37**(20), 4344–4346 (2012).
10. T. Meijer, J. D. White, B. Smeets, M. Jeppesen, and R. E. Scholten, "Blue five-level frequency-upconversion system in rubidium," Opt. Lett. **31**(7), 1002–1004 (2006).
11. A. Vernier, S. Franke-Arnold, E. Riis, and A. S. Arnold, "Enhanced frequency up-conversion in Rb vapor," Opt. Express **18**(16), 17020–17026 (2010).
12. J. F. Sell, M. A. Gearba, B. D. DePaola, and R. J. Knize, "Collimated blue and infrared beams generated by two-photon excitation in Rb vapor," Opt. Lett. **39**(3), 528–531 (2014).
13. R. C. Cao, B. G. Baodong Gai, J. Y. Jie Yang, T. L. Tong Liu, J. L. Jinbo Liu, S. H. Shu Hu, J. G. Jingwei Guo, Y. T. Yannan Tan, S. H. Shan He, W. L. Wanfa Liu, H. C. Hongxing Cai, and X. Z. and Xihe Zhang, "Efficient

#326433 https://doi.org/10.1364/OE.26.017254
Journal © 2018 Received 20 Mar 2018; revised 28 May 2018; accepted 28 May 2018; published 20 Jun 2018

Optics EXPRESS

generation of collimated frequency upconversion blue light in rubidium vapor," Chin. Opt. Lett. **13**(12), 121903 (2015).
14. R. Roy, P. C. Condylis, Y. J. Johnathan, and B. Hessmo, "Atomic frequency reference at 1033 nm for ytterbium (Yb)-doped fiber lasers and applications exploiting a rubidium (Rb) $5S_{1/2}$ to $4D_{5/2}$ one-colour two-photon transition," Opt. Express **25**(7), 7960–7969 (2017).
15. C. L. Collins, K. D. Bonin, and M. A. Kadar-Kallen, "Absolute two-photon cross section of Rb measured by differential absorption," Opt. Lett. **18**(20), 1754–1756 (1993).
16. C. V. Sulham, G. A. Pitz, and G. P. Perram, "Blue and infrared stimulated emission from alkali vapors pumped through two-photon absorption," Appl. Phys. B. **101**(1-2), 57–63 (2010).
17. Y. H. Chen, T. W. Liu, C. M. Wu, C. C. Lee, C. K. Lee, and W. Y. Cheng, "High-resolution ^{133}Cs 6S-6D, 6S-8S two-photon spectroscopy using an intracavity scheme," Opt. Lett. **36**(1), 76–78 (2011).
18. S. Shi, G. Chen, W. Zhao, and J. Liu, *Nonlinear Optica,* 2nd ed. (Xidian University, 2012), Chap. 5.
19. L. W. Tutt and T. F. Boggess, "A review of optical limiting mechanisms and devices using organics, fullerence, semiconductors, and other materials," Prog. Quantum Electron. **17**(4), 299–338 (1993).
20. G. S. He, L. Yuan, N. Cheng, J. D. Bhawalkar, P. N. Prasad, L. L. Brott, S. J. Clarson, and B. A. Reinhardt, "Nonlinear optical properties of a new chromophore," J. Opt. Soc. Am. B **14**(5), 1079–1087 (1997).
21. J. Heinrich and W. Behmenburg, "Two-photon resonant four-wave mixing processes in atomic barium," Appl. Phys. (Berl.) **23**(3), 333–339 (1980).
22. A. Smith and J. Ward, "Doubly Resonant Four-Photon Interactions in Cesium Vapor," IEEE J. Quantum Electron. **17**(4), 525–529 (1981).
23. G. A. Pitz and G. P. Perram, "Pressure broadening of the D1 and D2 lines in diode pumped alkali lasers," Proc. SPIE **7005**, 700526 (2008).
24. O. Axner, J. Gustafsson, N. Omenetto, and J. D. Winefordner, "Line strengths, -factors and absorption cross-sections for fine structure lines in multiplets and hyperfine structure components in lines in atomic spectrometry—a user's guide," Spectroc. Acta Pt. B-Atom. Spectr. **59**, 1–39 (2004).
25. T. William, *Laser Fundamentals,* 2nd ed. (Cambridge University, 2004), Chap. 4.
26. K. H. Weber and K. Niemax, "Self-broadening and shift of Doppler-free two-photon lines of Rb," Opt. Commun. **31**(1), 52–56 (1979).
27. C. E. Theodosiou, "Lifetimes of alkali-metal-atom Rydberg states," Phys. Rev. A **30**(6), 2881–2909 (1984).
28. W. Zapka, M. D. Levenson, F. M. Schellenberg, A. C. Tam, and G. C. Bjorklund, "Continuous-wave Doppler-free two-photon frequency-modulation spectroscopy in Rb vapor," Opt. Lett. **8**(1), 27–29 (1983).
29. F. Nez, F. Biraben, R. Felder, and Y. Millerioux, "Optical frequency determination of the hyperfine components of the $5S_{1/2}$-$5D_{3/2}$ two-photon transitions in rubidium," Opt. Commun. **102**(5-6), 432–438 (1993).

1. Introduction

Simultaneous two-photon absorption (2PA) has a broad range of applications in fluorescence microscopy, 3D optical memory, optical power limiting and photodynamic therapy since the first verified by Kaiser and Garret in 1961 [1–3]. And many theoretical and experimental research studies have been carried out in this field [4–6]. The two-photon absorption process of Rb has been paid more attention excitation in recent alkali vapor studies [7–10]. One of its advantages is the realization of cascading and coaxial output of blue-violet photons and mid-infrared photons, which can be used in many fields of military and scientific research, such as multi-wavelength detection, and atomic physics. Vernier achieved conversion efficiency of 2.6% in Rb by two-photon absorption experimentally in 2010 [11]. 420nm light with power of 9.1mW was obtained by two-photon excitation and the power efficiency was 1.5% in 2014 [12]. The energy efficiency over than 1% in Rb by single-wavelength conversion was realized in 2016 [13]. The research on new atomic transition frequency and spectroscopy of Rb which is realized by two-photon transition from the $5S_{1/2}$ to $4D_{5/2}$, was carried out in 2017 [14]. In order to quantitatively describe and analyze the absorption process, exact estimation of the 2PA spectra and the absorption cross-section values are of critical importance. Previously, Florescu used a modified precise one-electron model to calculate 2PA cross section of Rb $5S_{1/2}$-$5D_{5/2}$ as 0.57×10^{-26} m^4/W [6], and furthermore, Collins also measured the two-photon cross section for $5S_{1/2}(F = 2)$-$5D_{5/2}(F = 4)$ in ^{85}Rb by a differential absorption technique experimentally [15]. The spectral characteristics of 2PA of alkali vapor, such as Rb $5S_{1/2}$-5D, Cs 6S-8S and 6S-6D have been measured [16,17]. However, more unambiguous and systematic theory models are still needed to obtain the spectra and cross-section values of simultaneous two-photon cross section of Rb $5S_{1/2}$-5D.

Optics EXPRESS

In this paper, a theoretical study of the simultaneous two-photon excitation in the Rb four-wave mixing process is carried out. Based on the coupled-wave equation and definition of 2PA cross section, the intelligible expression of the 2PA in Rb four-wave mixing process is depicted and derived. The third-order susceptibility of Rb four-wave mixing process is calculated with the contribution of the intermediate $5P_{3/2}$, $5P_{1/2}$, $6P_{1/2}$ and $6P_{3/2}$ energy states. In addition, the nuclear spin and two isotopes of Rb are innovatively taken into account in four-wave mixing process with total angular momentum. The influences of hyperfine structures on 2PA cross section are analyzed, and the main reason of relatively low absorption efficiency is found out by comparing line shape spectrum of Rb absorption and profile of pumping light.

2. Description of the model

The Rb energy levels and four-wave mixing process with single-wavelength laser excitation are shown in Fig. 1. Due to small energy level spacing between $5D_{3/2}$ state and $5D_{5/2}$ state, and considering spectral linewidth of pumping laser and atom energy states, the Rb atoms can be excited to 5D states ($5D_{3/2}$ and $5D_{5/2}$ state) by 778.1nm two-photon absorption with the help of intermediate virtual level showed as dotted line in Fig. 1. For Rb four-wave mixing process, the atoms in $5D_{3/2}$ state radiate two kinds of photons with wavelengths of 5.24μm and 5.04μm to the states of $6P_{3/2}$ and $6P_{1/2}$ respectively, and the atoms in $5D_{5/2}$ state radiate photons with a wavelength of 5.23μm to $6P_{3/2}$ state. And then the blue-violet light of 420nm or 422nm from state of $6P_{3/2}$ or $6P_{1/2}$ back to ground state is radiated. The wave vectors of two pumping photons, the mid-infrared photon and the blue-violet photon are satisfied with phase-matching in the four-wave mixing process. The partial hyperfine structures are given in the right half of Fig. 1. The values in middle of two lines are energy differ of adjacent hyperfine structures. It should be noted that the two-photon absorption in our text refers to the excitation in the four-wave mixing process of Rb, which is different from ordinary two-photon absorption process.

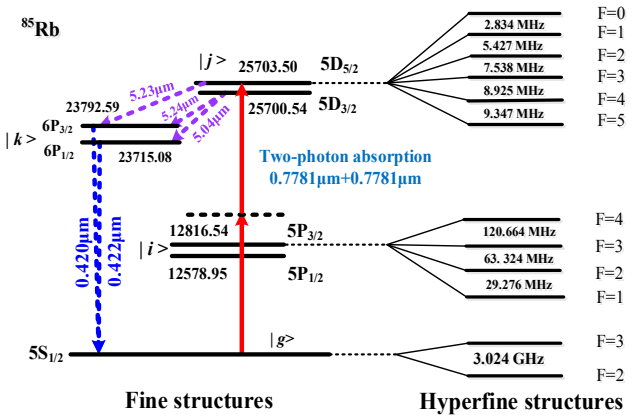

Fig. 1. Schematic illustration of energy structures and four-wave mixing process of ^{85}Rb.

Two photons of same frequency ν_P and pumping light intensity $I(\nu_P)$ are simultaneously absorbed by an Rb atom in its ground state leading to the excitation of 5D state. In coupled-wave equation of simultaneous two-photon absorption theory, pumping beam-intensity $I(\nu_P, z)$ change along the propagation direction (z axis) in Rb vapor cell can be expressed [18,19]

$$\frac{dI(\nu_P,z)}{dz} = -\frac{3\cdot(2\pi\cdot\nu_P)^3}{k_p^{\,2}c^2}\mu_0[I(\nu_P,z)]^2\,\mathrm{Im}[\chi^{(3)}]. \quad (1)$$

Optics EXPRESS

Where k_p is pumping laser wavenumber, and the speed of light in vacuum c is 3×10^8m/s. The permeability of vacuum μ_0 is $4\pi \times 10^{-7}$ H/m. Im[$\chi^{(3)}$] is the imaginary part of third-order susceptibility of Rb in four-wave mixing process, which relates to the 2PA.

The nonlinear absorption coefficient due to simultaneous two-photon absorption is defined by β [20], and corresponding 2PA cross sections σ_{TA} (in units of m^4/W) of the Rb atoms can be determined by using the similar solute molecules relationship [20]

$$\beta = \frac{3 \cdot (2\pi \cdot \nu_P)^3}{k_p{}^2 c^2} \mu_0 \, \mathrm{Im}[\chi^{(3)}] = \sigma_{TA} N. \tag{2}$$

$$\sigma_{TA} = \frac{3 \cdot 2\pi \cdot \nu_p}{n_p{}^2 N} \mu_0 \, \mathrm{Im}[\chi^{(3)}]. \tag{3}$$

Here N is atomic density. The n_p is the linear index of refraction. The σ_{TA} is proportional to frequency and imaginary part of third-order susceptibility.

To figure out the cross sections, we assume that incident pumping laser field is linearly polarized for simplification, and third-order susceptibility in four-wave mixing process is given by [21,22]

$$\chi^{(3)}(-\nu_{UV}, \nu_P, \nu_P, -\nu_{IR}) = \frac{Ne^4}{6\varepsilon_0 \pi h^3} \sum_{ijk} \frac{\mu_{gi}\mu_{ij}\mu_{jk}\mu_{kg}}{(\nu_i - \nu_P)(\nu_j - 2\nu_P - \mathrm{i}\Gamma_{gj})(\nu_k - \nu_{UV})} \rho_{gg}^{(0)}. \tag{4}$$

Where ν_{UV} and ν_{IR} are frequency of blue-violet light and mid-infrared light generated by four-wave mixing process, respectively, the ν_i, ν_j and ν_k are respectively transition frequency of 5S to 5P, 5S to 5D and 5S to 6P. The e is the electric charge and ε_0 is permittivity of vacuum. $\mu_{ij} = \langle n, s, j | r | n', s, j' \rangle$ is the electric-dipole matrix element between levels i and j, which is listed in Table 1. The Γ_{gi} reflects the linewidth of 5D energy level at frequency ν_p due to various broadening mechanisms. $\rho_{gg}^{(0)} = (2J_g + 1)^{-1}$ is the occupation probability of atomic state |g> showed in Fig. 1.

Table 1. Electric-dipole matrix elements[a] among levels *g*, *i*, *j* and *k*

μ	unit(10^{-10}m)	μ	unit(10^{-10}m)
$\mu_{5S_{1/2}-5P_{1/2}}$	2.2943	$\mu_{5D_{3/2}-6P_{3/2}}$	12.6249
$\mu_{5S_{1/2}-5P_{3/2}}$	3.2446	$\mu_{5D_{3/2}-6P_{3/2}}$	–4.2083
$\mu_{5P_{1/2}-5D_{3/2}}$	0.6233	$\mu_{5D_{3/2}-6P_{1/2}}$	9.4100
$\mu_{5P_{3/2}-5D_{5/2}}$	0.8362	$\mu_{6P_{3/2}-5S_{1/2}}$	–0.3544
$\mu_{5P_{3/2}-5D_{3/2}}$	0.2787	$\mu_{6P_{1/2}-5S_{1/2}}$	0.2506

[a]From IEEE J. Quantum Electron. **11**, 121-130 (1975).

To obtain the imaginary part of third-order susceptibility, the fine structures of 5D states need to be taken into consideration in Eq. (4) as

$$\begin{aligned} \mathrm{Im}[\chi^{(3)}(-\nu_{UV}, \nu_P, \nu_P, -\nu_{IR})] = {} & \frac{Ne^4 \rho_{gg}^{(0)}}{6\varepsilon_0 \pi h^3} \times \left[\frac{6\Gamma_{D_{5/2}}}{(\nu_{5D_{5/2}} - 2\nu_P)^2 + \Gamma_{D_{5/2}}{}^2}\right] \\ & + \left[\frac{4\Gamma_{D_{3/2}}}{(\nu_{5D_{3/2}} - 2\nu_P)^2 + \Gamma_{D_{3/2}}{}^2}\right] \times \sum_{ik} \frac{\mu_{gi}\mu_{ij}\mu_{jk}\mu_{kg}}{(\nu_i - \nu_P)(\nu_k - \nu_{UV})}. \end{aligned} \tag{5}$$

Here the coefficient 6 and 4 are degeneracy of $5D_{5/2}$ and $5D_{3/2}$, respectively. Σ is summation for the intermediate $5P_{1/2}$, $5P_{3/2}$, $6P_{1/2}$ and $6P_{3/2}$ states located between state |g>

Optics EXPRESS

and state $|j>$. Furthermore, for simultaneous two-photon absorption process, the influences of hyperfine structures (represent by the total angular momentum F) of states resulted from the coupling between electronic angular momentum **J** and the nuclear spin **I** (**I** = 3/2 for ^{87}Rb and **I** = 5/2 for ^{85}Rb) cannot be neglected. The hyperfine structures, shown in ^{85}Rb energy level diagram of Fig. 1, are described by the magnetic dipole ***A*** and electric quadrupole constant ***B***. Considering the influence of hyperfine structures, we innovatively borrow the thought from [23].Thus Eq. (5) is expanded as

$$\begin{aligned}\mathrm{Im}[\chi^{(3)}(-\nu_{UV},\nu_P,\nu_P,-\nu_{IR})] &= \frac{Ne^4\rho_{gg}^{(0)}}{6\varepsilon_0\pi h^3}\times\left[\frac{6\Gamma_{D_{5/2}}}{(\nu_{5D_{5/2}}-2\nu_P)^2+\Gamma_{D_{5/2}}{}^2}\right] \\ +\left[\frac{4\Gamma_{D_{3/2}}}{(\nu_{5D_{3/2}}-2\nu_P)^2+\Gamma_{D_{3/2}}{}^2}\right]&\times\sum_{ik}\frac{\mu_{gi}\mu_{ij}\mu_{jk}\mu_{kg}}{(\nu_i-\nu_P)(\nu_k-\nu_{UV})}\times S_{FF''}\times f_{iso}\times f_F,\end{aligned} \tag{6}$$

where f_{iso} is relative natural abundance (^{85}Rb 72.2%; ^{87}Rb 27.8%) and f_F is statistical distribution of population among F states of $5S_{1/2}$ energy level, which can be given by

$$f_F = \frac{(2\mathrm{F}+1)\mathrm{e}^{-E(F)/\mathrm{kT}}}{\sum_F(2\mathrm{F}+1)\mathrm{e}^{-E(F)/\mathrm{kT}}}. \tag{7}$$

The hyperfine line strengths $S_{FF''}$ specifies relative intensities of the F→F″ (5S-5D) transitions of the two Rb isotopes, which represents the relative probability of transitions among hyperfine states. The $S_{FF''}$ is expressed as [24]

$$\mathrm{S}_{FF''} = (2F''+1)(2J+1)\begin{Bmatrix} J & J'' & 1 \\ F'' & F & 1\end{Bmatrix}^2. \tag{8}$$

The hyperfine line strengths and the frequency offset from center frequency are listed in Table 2. It contains all possibilities of two-photon hyperfine transition from ground state $5S_{1/2}$ to 5D in two Rb isotopes. The center frequency corresponds to the transition frequency between $5S_{1/2}$ and 5D in Fig. 1 when only fine structures are considered. And a summary of other critical parameters used in the calculation are listed in Table 3. The former two parameters are calculated according to the data in [16], and the another two parameters are valued when the ν_{UV} is set up as intermediate value of $\nu_{6P1/2}$ and $\nu_{6P3/2}$.

Table 2. Hyperfine line strengths and the frequency offset from center frequency [a,b]

^{85}Rb			^{87}Rb		
$5S_{1/2}$-$5D_{3/2}$	$S_{FF''}$	frequency offset $\Delta\nu$(MHz)	$5S_{1/2}$-$5D_{3/2}$	$S_{FF''}$	frequency offset $\Delta\nu$(MHz)
F = 2 F = 2	0.2017	1756.90	F = 1 F = 1	0.2501	4232.03
F = 2 F = 4	0.3469	1726.68	F = 1 F = 3	0.3749	4304.56
F = 3 F = 1	0.1157	–1232.49	F = 2 F = 0	0.3214	–2616.24
F = 3 F = 3	0.3356	–1216.16	F = 2 F = 4	0.0536	–2574.59
$5S_{1/2}$-$5D_{5/2}$	$S_{FF''}$	frequency offset $\Delta\nu$(MHz)	$5S_{1/2}$-$5D_{5/2}$	$S_{FF''}$	frequency offset $\Delta\nu$(MHz)
F = 2 F = 0	0.0667	1791.85	F = 1 F = 1	0.2011	4311.93
F = 2 F = 2	0.0934	1783.58	F = 1 F = 3	0.2110	4272.18
F = 2 F = 4	0.1999	1767.12	F = 2 F = 2	0.1003	–2538.76
			F = 2 F = 4	0.5022	–2590.77
F = 3 F = 1	0.0055	–1235.08			
F = 3 F = 3	0.2342	–1222.12			
F = 3 F = 5	0.5239	–1203.85			

[a]From Spectroc. Acta Pt. B-Atom. Spectr. **59**, 1-39 (2004).
[b]From Rev. Mod. Phys **49**, 31-76 (1977).

Optics EXPRESS

Table 3. Summary of other critical parameters in model

Parameter Symbol	Value	Reference
$v_{5P_{1/2}} - v_P$	-8.16×10^{12} Hz	[16]
$v_{5P_{3/2}} - v_P$	-1.06×10^{12} Hz	[16]
$v_{6P_{1/2}} - v_{UV}$	-1.20×10^{12} Hz	This work
$v_{6P_{3/2}} - v_{UV}$	1.20×10^{12} Hz	This work

3. Result and discussions

The linewidth Γ_{gi} of 5D states is related to many factors such as temperature of vapor, buffer gas. The influences of buffer gas are neglected for lacking of relevant experimental data. The parameter Γ_{gi} exists different values when Rb vapor is excited by single-wavelength pumping beam in two different ways, which are only co-propagating laser beam, and both co- and counter-propagating laser beams equally existence, respectively. In the first case, the Γ_{gi} is determined by the Doppler broadening of energy level, which is about 1.2GHz calculated by formula of Gauss linewidth [25] when the temperature of Rb vapor is supposed to 443K. In the other case, in order to study the influence of narrow linewidth Γ_{gi} on the cross section σ_{TA}, we suppose that the co- and counter-propagating laser beams are separated by minimum angle (several milliradians) which is to ensure the phase-matching. And we still think that the first-order Doppler effect is eliminated considering of the minimum angle of co- and counter-propagating laser beams, so the main contribution to the linewidth Γ_{gi} is excited-state lifetime and linewidth caused by collisions within Rb atoms is ignored [26]. The linewidth Γ_{gi} of the excited $5D_{5/2}$ state and $5D_{3/2}$ state are approximately 1.5MHz calculated by the excited-state lifetime with 230 ± 23 ns [27].

Optics EXPRESS

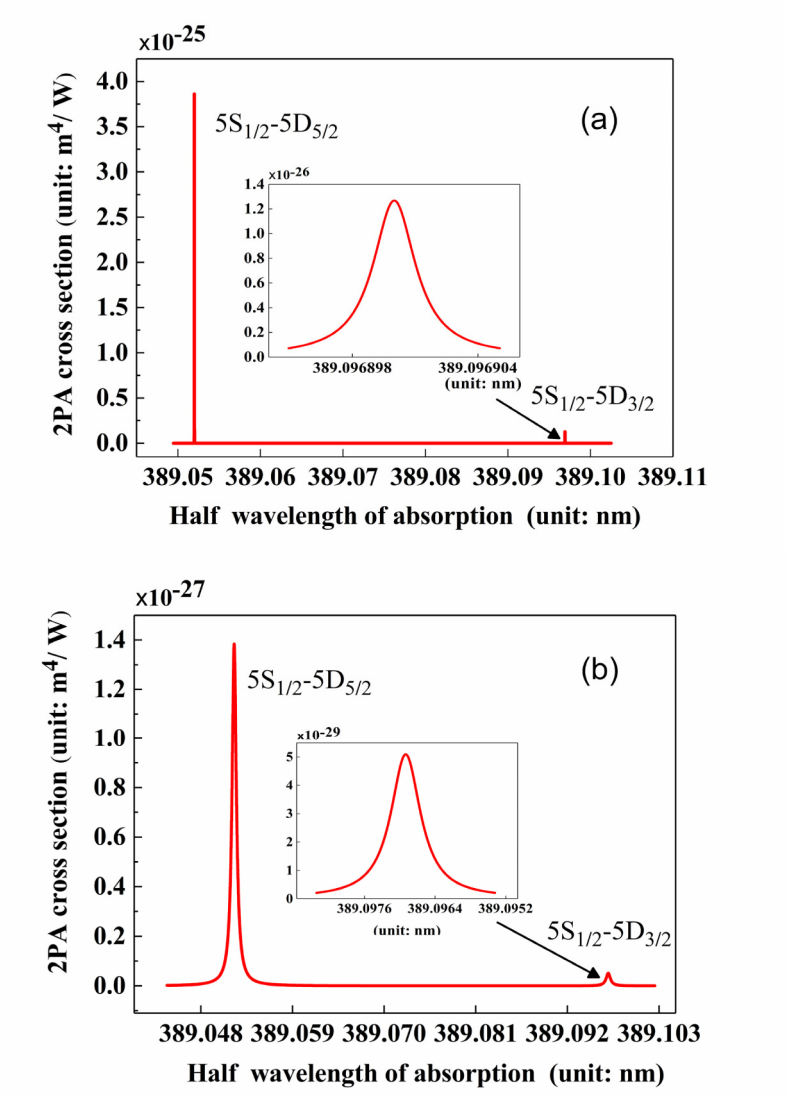

Fig. 2. The cross section of two-photon absorption σ_{TA} versus half wavelength of absorption. (a) only co-propagating laser beam exist with linewidth 1.5MHz. (b) co- and counter-propagating laser beams equally existence with linewidth 1.2GHz.

The cross section of two-photon absorption σ_{TA} can be obtained by substituting Eq. (5) into Eq. (3) with different values of Γ_{gi}. The results are shown in Fig. 2. The σ_{TA} nearly become vertical line in Fig. 2(a) for the very narrow linewidth of 5D level about 1.5MHz, and partial enlarged drawing is located in the middle. The σ_{TA} of $5S_{1/2}$-$5D_{5/2}$ transition is about 26 times larger than that of $5S_{1/2}$-$5D_{3/2}$, which is collectively determined by two parameters μ and ν_{5P}-ν_P (transition frequency difference between the 5P state and intermediate virtual state) listed in Table 1 and Table 3, respectively. Therefore, it is efficient to elect the $5D_{5/2}$ state as the upper level. As shown in Figs. 2(a) and 2(b), there has different σ_{TA} of $5S_{1/2}$-$5D_{5/2}$ transition when two distinct pumping schemes are taken into account. According to Eq. (5), the maximum cross section is inversely proportional to linewidth Γ_{gi}, and therefore the σ_{TA} of $5S_{1/2}$-$5D_{5/2}$ in Fig. 2(a) is larger orders of magnitude than that in Fig. 2(b). It can be seen that the maximum σ_{TA} about 2.5×10^{-26} m^4/W in Fig. 2(a) is too small, and the result suggests that

Optics EXPRESS

there must be high pumping power intensity comparing with single photon-atom interaction transition, which will be restricted in applications.

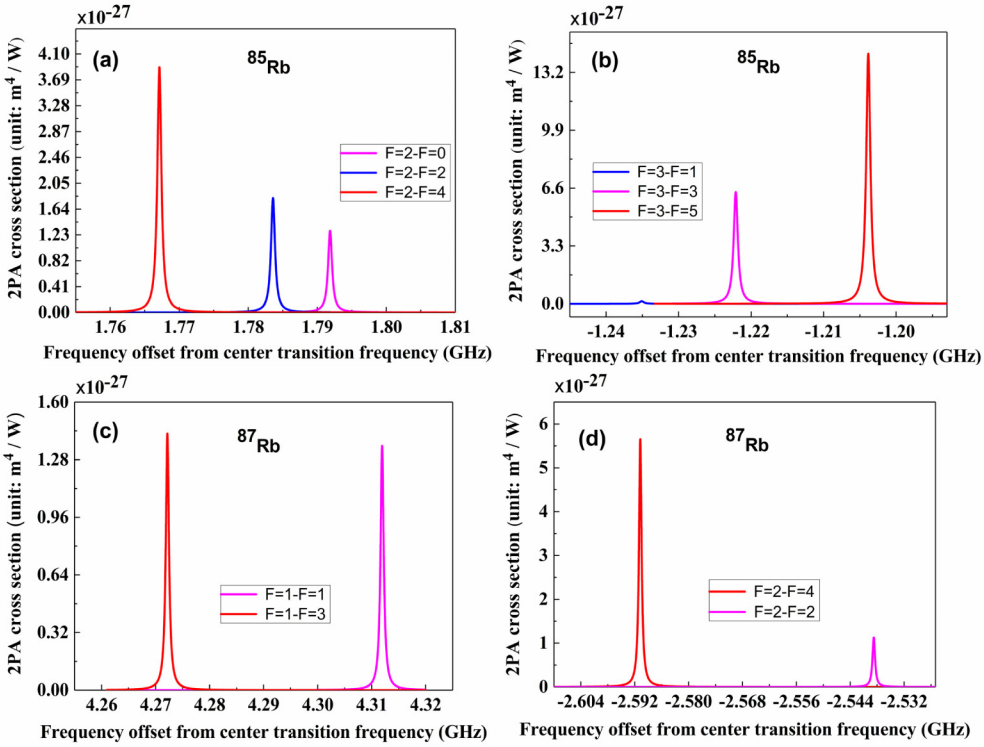

Fig. 3. (a)-(b) The 2PA cross sections of $5S_{1/2}$-$5D_{5/2}$ hyperfine transition of ^{85}Rb versus the frequency offset from center transition frequency when the linewidth Γ_{gi} of $5D_{5/2}$ is 1.5MHz; (c)-(d) the 2PA cross sections of $5S_{1/2}$-$5D_{5/2}$ hyperfine transition of ^{87}Rb versus the frequency offset from center transition frequency when the linewidth Γ_{gi} of $5D_{5/2}$ is 1.5MHz.

The influences of hyperfine structures on two-photon excitation are analyzed. As shown in Fig. 2, the σ_{TA} of $5S_{1/2}$-$5D_{5/2}$ transition is far larger than that of $5S_{1/2}$-$5D_{3/2}$, so we neglect the influence of $5S_{1/2}$-$5D_{3/2}$ transition to the σ_{TA}. The linewidth Γ_{gi} of $5D_{5/2}$ level is about 1.5MHz when co- and counter-propagating laser beams equivalently coexist. The linewidth of $5D_{5/2}$ level is relatively smaller compared with the energy difference of hyperfine structures, so the influences of these hyperfine structures are obvious. It is shown in Figs. 3(a)-3(d) that the 2PA cross sections of $5S_{1/2}$-$5D_{5/2}$ transition of Rb isotopes versus the frequency offset from center transition frequency. From Fig. 3, two isotopes have distinct hyperfine structures for each state and transitions of two-photon absorption obey the rule $|\Delta F| = 0, \pm 2$. The superior of σ_{TA} for ^{85}Rb and ^{87}Rb is transition of F = 3-F = 5 and F = 2-F = 4, which are respectively correspond to transition between the higher F of ground $5S_{1/2}$ state and terminal $5D_{5/2}$ state. We deduce that the reason of larger σ_{TA} between higher hyperfine transitions might result from more atoms accumulating in higher F of ground $5S_{1/2}$ state according to the Eq. (7). And the σ_{TA} gradually reduces from the higher hyperfine structure F to lower F of $5D_{5/2}$ state for ^{85}Rb and ^{87}Rb. However, frequency offset are significant differences between ^{85}Rb and ^{87}Rb.

In order to validate the results, we compare our simulation results with some experimental values reported so far. Zapka et al. have experimentally measured the value of σ_{TA} of $5S_{1/2}$(F = 2)→$5D_{5/2}$(F = 4) transition in ^{87}Rb and the value is 4×10^{-28} m^4/W [28]. Our calculated result of σ_{TA} for ^{87}Rb in Fig. 3(d) is about 5.9×10^{-27} m^4/W which remains within the error

Optics EXPRESS

range caused by different linewidth Γ_{gi} in distinct experimental circumstances. The maximum σ_{TA} of ^{85}Rb $5S_{1/2}$-$5D_{5/2}$ is hyperfine transition of F = 3-F = 5 with 1.41×10^{-26} m^4/W in Fig. 3(b), which is close to the 2PA cross section of Rb $5S_{1/2}$-$5D_{5/2}$ as 0.57×10^{-26} m^4/W in [6] and the experimentally measured value of $(1.2 \pm 0.5) \times 10^{-26}$ m^4/W in [15]. And in addition, Nez et al. have experimentally measured the absolute frequencies and relative strength of hyperfine structure of the $5S_{1/2}$-$5D_{5/2}$ two-photon transition in rubidium [29]. By comparison, our calculated results agree well with the experimental outcomes reported in [29] both relative height and frequency interval of each hyperfine energy level transition.

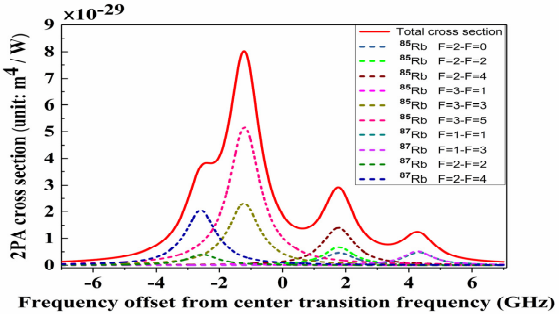

Fig. 4. The 2PA cross sections of $5S_{1/2}$-$5D_{5/2}$ hyperfine transition versus the frequency offset from center transition frequency when the linewidth Γ_{gi} of $5D_{5/2}$ is 1.2GHz. The solid line refers to total absorption cross section, and every dotted line refers to one hyperfine transition in two Rb isotopes.

The 2PA cross section σ_{TA} of $5S_{1/2}$-$5D_{5/2}$ hyperfine transition versus the frequency offset from center transition frequency in Fig. 4 when the linewidth Γ_{gi} is 1.2GHz. The lineshape of total absorption cross section is a whole for wide linewidth of every hyperfine structure. It can be seen that the σ_{TA} has four main peaks in Fig. 4. The two peaks closed to center transition frequency are caused by hyperfine transition in ^{85}Rb, and the other two peaks are caused by transition in ^{87}Rb. The total absorption cross section covers up more details about the intensity and number of hyperfine transition. Moreover, the value of σ_{TA} in Fig. 4 is much smaller comparing with Fig. 3, which results from cross section is inversely proportional to linewidth Γ_{gi} of 5D state.

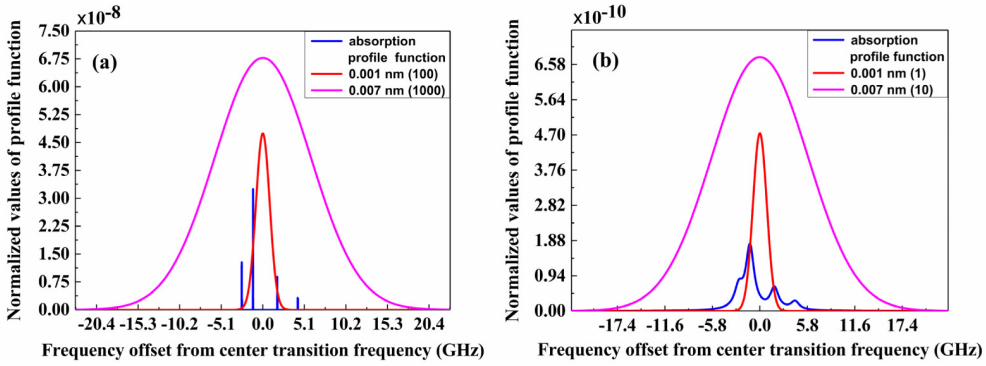

Fig. 5. Normalized profile function of pumping beam and two-photon absorption process when hyperfine structures are taken into account. The values in brackets of diagrams are the expanded multiple of pumping beam for comparing with absorption profile function. (a) linewidth of absorption profile function is 1.5MHz. (b) linewidth of absorption profile function is 1.2GHz.

The narrow linewidth of two-photon absorption process of 5D level in Rb have a great help to spectral resolution and measurement. However, it is also the disadvantage of high

Optics EXPRESS

absorption efficiency. As shown before, two pumping schemes not only affect the absorption linewidth, but have an impact on the σ_{TA}. To analyze the influence of linewidth on absorption process when hyperfine structures are taken into account, normalized profile function of pumping beam and two-photon absorption linewidth according to former results are shown in Fig. 5. It is shown that Figs. 5(a) and 5(b) are normalized profile function of linewidth Γ_{gi} with 1.5MHz and 1.2GHz, respectively. The profile function of pumping beam is considered as Gaussian lineshape and linewidth is set up as 0.001nm or 0.007nm. It can be seen from Fig. 5 that the two absorption lineshapes are quite different that depend on pumping schemes. The ratio of overlap of pumping lineshape and absorption lineshape increase as linewidth of pumping beam reduces, and absorption profile is beyond pumping spectrum range when linewidth of pumping beam is 0.001nm. From Fig. 5(b), hyperfine transition is indistinguishable because of larger linewidth, and the normalized profile is much smaller than that of Fig. 5(a). Moreover, red shift about 1.1GHz of frequency for pumping light could increase the overlap of pumping lineshape and absorption lineshape to obtain large absorption rate.

As we all know, wide absorption linewidth is guarantee of high absorption efficiency for the laser gain medium. If two-photon excitation of Rb vapor is used as laser medium, the problem of linewidth matching between medium absorption and pumping beam need to be solved. We can know that there are two ways to improve the problem from Fig. 5. One is linewidth narrowing of pumping beam by volume grating. However, it has the minimum limitation from Fig. 5. And it also needs to balance the relationship of narrow linewidth and large pumping power intensity. The other way is appropriate buffer gas filled in vapor to wide absorption linewidth. But more experiment data about influences of buffer gas to two-photon absorption is needed. Combining two ways might be an effective method to solve the problem.

4. Conclusion

In this study, we report an absorption cross section model in Rb simultaneous two-photon excitation process. The absorption cross section σ_{TA} is calculated when the hyperfine structures of two isotopes are taken into account. The calculated results show that it is efficient to elect the $5D_{5/2}$ state as the upper level for the σ_{TA} of $5S_{1/2}$-$5D_{5/2}$ transition being far larger than that of $5S_{1/2}$-$5D_{3/2}$, and it is essential to pumping Rb vapor using extremely strong pumping power intensity for simultaneous two-photon excitation process. In addition, hyperfine structures have an important influence on the σ_{TA} value and profile for simultaneous two-photon absorption. The model and simulation results of σ_{TA} could provide support for study and design in simultaneous two-photon absorption process. Two ways, linewidth narrowness of the pumping beam and absorption linewidth broadening by appropriate buffer gas filled, are proposed to improve absorption efficiency. The influences of types and amount of buffer gas need to be more researched in the future study.

Funding

The National Defense Science and Technology Innovation Fund of the Chinese Academy of Sciences (Grant No.CXJJ-16M228); the Major Science and Technology Biding Project of Jilin Province (No.20160203016GX); the Young and Middle-Aged Science and Technology Innovation Leader and Team Project of Jilin Province (No.2017051901JH); and the Youth Innovation Promotion Association of CAS (No. 2017259).